formation of the main deposit. At lower current densities, it is possible to deposit only this extremely thin tin film: it is 5 nm thick (Fig. 4), and composed of a carpet of small grains side by side. Whereas the 200-nm copper and 300-nm tin films in Fig. 4 have a thickness close to that predicted by theory, the 5-nm film is much thinner.

We expect that the deposition reported here will be possible with any metal that is known to deposit in the powdery regime of growth, in the shape of rounded crystals. We propose the following mechanistic explanation of this effect. First, in thin cells, and with a binary electrolyte, very high fields are generated at the tips of the deposits[17]. These very high fields induce nucleation and growth of a polycrystalline deposit[19]. As it is observed that growth is much more rapid in scratches[5,20], it is clear that the dangling bonds of glass have catalytic properties, under the action of the large electric field. We now consider why the deposit should be covering for higher currents. As seen in Fig. 2, this surprising stability is not due to an increase in the size of deposit features up to the sample size, but to a progressive closing of voids between ever-smaller branches, in which individual grains become themselves ever smaller[19]. This proves that, as the growth speed is increased, the capillary length of individual branches is decreased (as expected from theory[9,23]). But so is the typical size λ of gradients ahead of the deposit, because[16] $\lambda = (-kT/eE_0)(z_c + z_a)(z_c z_a)(1 + \mu_a/\mu_c)$, where E_0 is the electric field in the bulk, and z_c, z_a, μ_c and μ_a are the charges and mobilities of the cations and anions. When λ becomes smaller than the grain size, instabilities cannot develop, and the front is stable ('absolute stability' in the context of pattern formation). This stability makes it possible to electroplate insulators in conditions very far from equilibrium. The coating of fibres, ribbons and plates seems possible. Many applications of this process may be considered, such as replacing the vapour seeding process in the electronics industry, tailoring mirrors of unusual metals or shapes, and direct coating of organic materials. In general terms, the process proposed here has some advantages over conventional electroless deposition on insulators, in that the film progression and grain size are controlled externally, the process can be interrupted at any time, and it should work with many simple salts, even without additives. But it should be acknowledged that, as the deposition process starts from one end of the sample and progresses towards the other end at speeds of the order of $1\,m\,h^{-1}$ at most, the overall production output would be much smaller than existing electroless techniques, which coat in approximately 5 minutes glass plates of size $4\,m \times 4\,m$.

We note that using this very rapid plating technique with Li, as reported here for Ag, Cu and Sn, might eliminate the cycling problems of Li rechargeable batteries. Indeed, cycling efficiency of Li batteries is drastically reduced by dendritic growth. This is ascribed, in part, to the poor cyclability of a powdery tree. In present designs, dendrites are always seen to grow perpendicularly to the electrodes. A set-up similar to ours would in principle generate a thin film whose morphology is easier to cycle. □

Received 30 April 2001; accepted 25 February 2002.

1. Dini, J. *Electrodeposition* (Noyes Publication, Park Ridge, New Jersey, 1992).
2. Kircher, A. *Mundus Subterraneus, Caput VI, liber duodecimus part I*, Ars Chymurgica (Apud Janssonium et Weyerstraten, Amsterdam, 1664).
3. Kircher, A. *China Monumentis qua Sacris qua Profanis, nec non Variis Naturae et Artis Spectaculis Aliarumque Rerim Meomriabilium Argumentis Illustrata* (Apud Janssonium et Weyerstraten, Amsterdam, 1667).
4. Needham, J. & Peng Yoke, H. *Science and Civilization in China* **Vol. 5(2) (Cambridge Univ. Press,** Cambridge, 1984).
5. Fleury, V. *Arbres de Pierre, La Croissance Fractale de la Matière* (Flammarion, Paris, 1998).
6. Fleury, V. Patent PCT/FR00/02757 (2000).
7. Bergstrasser, T. R. & Merchant, H. D. in *Defect Structure, Morphology and Properties of Deposits Proceedings of the Materials Week Rosemont 1994* (ed. Merchant, H. D.) 115–168 (Minerals Metals Materials Society, Warrendale, Pennsylvania, 1995).
8. Despic, A. R. & Popov, K. I. in *Modern Aspects of Electrochemistry* **Vol. 7 (eds Conway,** B. E. & Bockris, J. O'M.) 199–313 (Butterworths, London, 1972).
9. Pelcé, P. *Dynamics of Curved Fronts* (Academic, London, 1991).
10. Meakin, P. *Fractals, Scaling and Growth far from Equilibrium* (Cambridge Univ. Press, Cambridge, 1988).
11. Vicsek, T. *Fractal Growth Phenomena* 2nd edn (World Scientific, Singapore, 1992).
12. Matsushita, M., Sano, M., Hayakawa, Y., Honjo, H. & Sawada, Y. Fractal structure of zinc metal leaves grown by electrodeposition. *Phys. Rev. Lett.* **53,** 286–289 (1984).
13. Fleury, V., Chazalviel, J. N., Rosso, M. & Sapoval, B. The role of the anions in the growth speed of electrochemical deposits. *J. Electroanal. Chem.* **290,** 249–255 (1990).
14. Melrose, J. R., Hibbert, D. B. & Ball, R. C. Interfacial velocity in electrochemical deposition and the Hecker effect. *Phys. Rev. Lett.* **65,** 3009–3012 (1990).
15. Garik, P. *et al.* Laplace and diffusion controlled growth in electrochemical deposition. *Phys. Rev. Lett.* **62,** 2703–2706 (1989).
16. Chazalviel, J. N. Electrochemical aspects of the generation of ramified metallic deposits. *Phys. Rev. A* **42,** 7355–7367 (1990).
17. Fleury, V., Chazalviel, J. N., Rosso, M. & Sapoval, B. Experimental aspects of dense morphology in copper electrodeposition. *Phys. Rev. A* **44,** 6693–6705 (1991).
18. Fleury, V. On a new kind of ramified electrodeposits. *J. Mater. Res. Soc.* **6,** 1169–1174 (1991).
19. Fleury, V. Branched fractal patterns in non-equilibrium electrochemical deposition from oscillatory nucleation and growth. *Nature* **390,** 145–148 (1997).
20. Fleury, V. & Barkey, D. Runaway growth in two-dimensional electrodeposition. *Europhys. Lett.* **36,** 253–258 (1996).
21. Rosso, M., Chazalviel, J. N., Fleury, V. & Chassaing, E. Experimental evidence for gravity induced motion in the vicinity of ramified electrodeposits. *Electrochim. Acta* **39,** 507–515 (1994).
22. Chazalviel, J. N., Rosso, M., Chassaing, E. & Fleury, V. A quantitative study of gravity-induced convection in two-dimensional parallel electrodeposition cells. *J. Electroanal. Chem.* **407,** 61–73 (1996).
23. Ben-Jacob, E. & Garik, P. The formation of patterns in non-equilibrium growth. *Nature* **343,** 523–530 (1990).

Acknowledgements

W.A.W. acknowledges the financial support of Saint-Gobain.

Correspondence and requests for materials should be addressed to V.F. (e-mail: vincent.fleury@polytechnique.fr).

Constraints on radiative forcing and future climate change from observations and climate model ensembles

Reto Knutti, Thomas F. Stocker, Fortunat Joos & Gian-Kasper Plattner

Climate and Environmental Physics, Physics Institute, University of Bern, Sidlerstr. 5, 3012 Bern, Switzerland

The assessment of uncertainties in global warming projections is often based on expert judgement, because a number of key variables in climate change are poorly quantified. In particular, the sensitivity of climate to changing greenhouse-gas concentrations in the atmosphere and the radiative forcing effects by aerosols are not well constrained, leading to large uncertainties in global warming simulations[1]. Here we present a Monte Carlo approach to produce probabilistic climate projections, using a climate model of reduced complexity. The uncertainties in the input parameters and in the model itself are taken into account, and past observations of oceanic and atmospheric warming are used to constrain the range of realistic model responses. We obtain a probability density function for the present-day total radiative forcing, giving 1.4 to 2.4 $W\,m^{-2}$ for the 5–95 per cent confidence range, narrowing the global-mean indirect aerosol effect to the range of 0 to –1.2 $W\,m^{-2}$. Ensemble simulations for two illustrative emission scenarios suggest a 40 per cent probability that global-mean surface temperature increase will exceed the range predicted by the Intergovernmental Panel on Climate Change (IPCC), but only a 5 per cent probability that warming will fall below that range.

The expected future warming of the climate system and its potential consequences increase the need for climate projections with clearly defined uncertainties and likelihood estimates[2]. The IPCC provides these probabilities for most of their findings in the

recently published Third Assessment Report[1]. However, some of the most important uncertainties—such as the projected surface warming—are still based on expert judgement, and are only given as ranges derived from different models. The evidence that part of the observed warming of both atmosphere and ocean[3,4] is caused by anthropogenic emissions of greenhouse gases and aerosols[1,5–10] may help assess climate models, and has been used to scale model projections for the next few decades[11,12]. Wigley and Raper[13] recently presented probabilities for the future warming by performing ensemble simulations with a simplified model calibrated to the same three-dimensional (3D) ocean–atmosphere models as used in the IPCC Third Assessment Report[1]. The combination of ensemble simulations that take into account uncertainties in input and model parameters with the use of observational evidence as an independent constraint provides a powerful approach for an objective uncertainty assessment in global warming projections. Here we determine constraints on the climate sensitivity, on the radiative forcing and on the future warming that arise from the requirement that the modelled large-scale surface warming and ocean heat uptake both match observations. We do this by using the reconstructed and projected radiative forcing of all major forcing components in combination with ensemble simulations of a coupled ocean–atmosphere model of reduced complexity (see Methods section).

To illustrate the relationship between radiative forcing, climate sensitivity, ocean mixing and the resulting model response, we have first calculated the global ocean heat uptake (Fig. 1a) and global-mean surface warming (Fig. 1b) for various set-ups of the ocean model and climate sensitivities. In this study, climate sensitivity is expressed as the increase of global-mean equilibrium surface temperature for a doubling of pre-industrial atmospheric CO_2 concentration. The mean and standard deviation of all model simulations (Fig. 1a and b, solid lines and shaded bands) denote the uncertainty in ocean heat uptake and surface warming due to ocean model uncertainties in mixing properties and surface-to-depth transport of excess heat, an important variable affecting the transient temperature trend[14]. This allows us to test recent claims by Barnett *et al.*[10] that observed ocean heat uptake provides the strongest constraint on the climate sensitivity and that climate sensitivity has to be low in order to match the observed ocean heat uptake. However, in their 3D simulations, Barnett *et al.* neglect the radiative effects of changes in solar irradiance, volcanic aerosols and the indirect effect of aerosols, as well as the uncertainties that are attached to the observed ocean heat uptake and surface warming. Taking all these factors into account, we find that climate sensitivity is only weakly constrained by the observed ocean heat uptake.

The comparison of the modelled ocean heat uptake with the instrumental estimates (Fig. 1a, horizontal solid lines) and their uncertainties (one standard deviation, horizontal dotted lines)[4] yields an approximate climate sensitivity of 5.7 K, with an uncertainty of ±1 K attributable to model uncertainties and ±2 K due to uncertainties in the data. The same diagnostics for the modelled surface temperature increase over the last century and the observed surface warming of 0.6 ± 0.1 K (ref. 2) yields a climate sensitivity of 4.6 K with uncertainties of about −1.5 to +1.5 K attributable to model uncertainties, and −1.3 to +2.6 K due to uncertainties in the data (Fig. 1b). Additional uncertainties arise from uncertainties in radiative forcing. The global-mean indirect aerosol forcing, for example, is estimated by IPCC[1] to be in the range of 0 to $-2\,W\,m^{-2}$ for the year 2000. We have performed simulations where either the indirect aerosol effect (Fig. 1c and d, dash-dotted) or the natural (solar and volcanic) forcings (Fig. 1c and d, dashed)

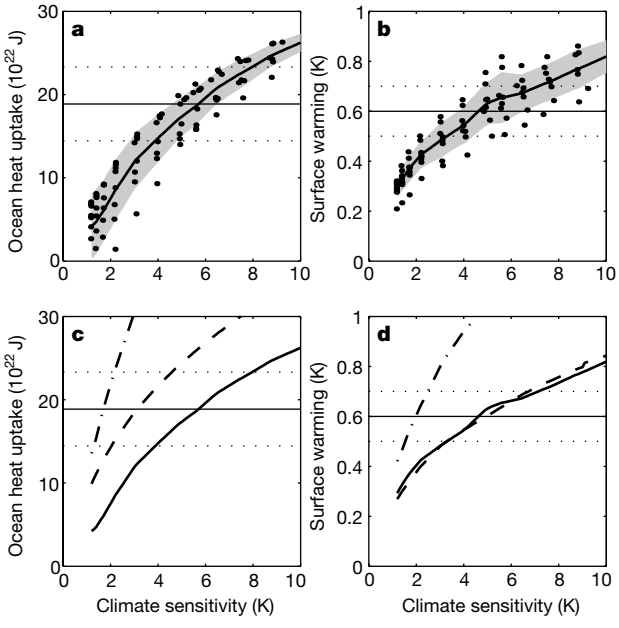

Figure 1 Relation between radiative forcing, climate sensitivity, and modelled atmospheric and oceanic warming. **a**,**b**, Global ocean heat uptake 1955–95 (to a depth of 3,000 m) and global-mean surface air temperature increase 1900–2000 versus climate sensitivity (expressed as global-mean equilibrium surface temperature increase for a doubling of pre-industrial atmospheric CO_2) for eight model set-ups (different subgrid-scale mixing parameterizations[29] and different vertical diffusivities). Calculations were performed using standard reconstructed anthropogenic and natural radiative forcing. Each dot indicates one model simulation. The bold solid curve and shaded band denote the mean and uncertainty (one standard deviation) arising from different ocean mixing properties. Horizontal solid and dotted lines mark the mean and uncertainty (one standard deviation) of the observed ocean heat uptake[4] and observed surface temperature increase[3]. **c**,**d**, Model mean values as in **a** and **b** (solid lines), but when neglecting natural, that is, solar and volcanic, forcings (dashed lines) or when neglecting the indirect aerosol forcing (dash-dotted lines). Constraining the climate sensitivity from the observed warming is mainly hampered by uncertainties in the radiative forcing components and temperature data rather than by the range covered by various set-ups of the climate model used.

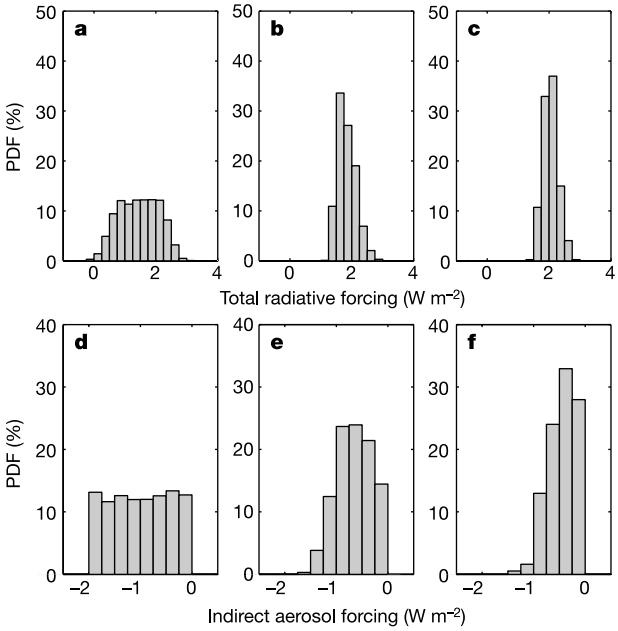

Figure 2 Constraints on the radiative forcing from the observed atmospheric and oceanic warming. Probability density functions (PDF) for the total (anthropogenic and natural) radiative forcing (**a**–**c**) and the indirect aerosol forcing (**d**–**f**) in the year 2000 are based on 25,000 Monte Carlo simulations. The initially assumed PDFs are given in **a** and **d**. The requirement that the model matches the temperature observations strongly narrows the PDFs (**b** and **e**). If in addition the climate sensitivity is restricted to the range adopted by the IPCC (1.5–4.5 K), the PDFs in **c** and **f** are obtained.

were neglected. Low estimates for climate sensitivity result from ignoring the indirect aerosol effect, whereas high climate sensitivities are required to match observations when assuming a strong indirect aerosol effect.

From Fig. 1c and d we estimate a climate sensitivity of about 6 K required to match the observed warming trend when applying anthropogenic and natural forcings. Similarly, about 4 K and 2 K are appropriate when neglecting natural forcings or the indirect aerosol effect. The evolution with time of surface warming and ocean heat uptake for these three forcing cases and the standard ocean model set-up shows that the model is able to reasonably reproduce the observed temporal evolution of global-mean surface warming[3] for the past 140 years with and without the indirect aerosol forcing (see Supplementary Information). The model has difficulties in reproducing the almost constant temperature between 1940 and 1970 and the strong warming after 1980, indicating that either the assumed radiative forcing is not correct, or part of the observed temperature evolution is due to internal climate variability which is not resolved in this model. When the natural forcing is neglected, much of the variability in the surface warming is lost and

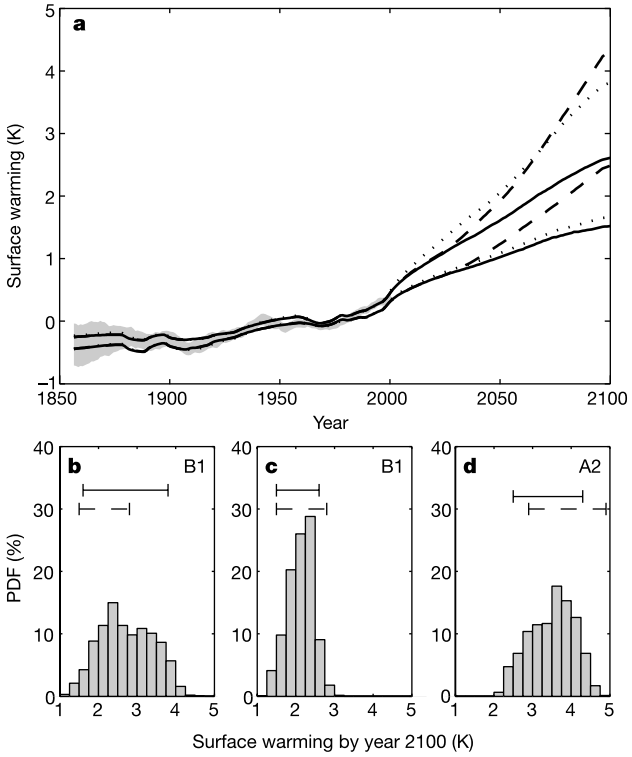

Figure 3 Probabilistic surface warming projections for two IPCC scenarios, as constrained by the observed atmospheric and oceanic warming. **a**, Range (5–95%) of projected global-mean surface air temperature increase (10-yr running mean) for the IPCC SRES illustrative emission scenarios B1 (solid lines, dotted lines) and A2 (dashed lines). Results are obtained from those ensemble members that match observed surface warming (grey shaded band) and observed ocean heat uptake (not shown), for climate sensitivities of 1–10 K (dotted lines for scenario B1) or for the IPCC range 1.5–4.5 K (solid lines for scenario B1, dashed lines for scenario A2). Panels **b**–**d** show the corresponding PDFs for the surface warming by year 2100. Confidence ranges (5–95%) based on the PDFs, and the uncertainties proposed by IPCC[1], are given as solid and dashed horizontal bars, respectively. When the observed warming is taken as the only constraint, the projected range for scenario B1 largely exceeds the uncertainties given by the IPCC (**b**, and dotted lines in **a**), indicating that currently accepted projections strongly rely on model-derived climate sensitivities and might underestimate the probability of a strong warming. If the range of climate sensitivity is independently constrained (1.5–4.5 K), our 5–95% estimates roughly agree with the uncertainty proposed by the IPCC for scenario B1 (**c**, and solid lines in **a**), and for A2 (**d**, and dashed lines in **a**).

the agreement is significantly worse, consistent with earlier model studies[6,7,9]. This applies similarly to the modelled ocean heat uptake, except that much less of the decadal structure in the data[4] is reproduced, consistent with results obtained with 3D models[10,15].

To attach probabilities to our results, we have simulated a Monte Carlo set of 25,000 global warming simulations using five ocean model set-ups and taking into account the uncertainties in radiative forcings and climate sensitivity (see Methods section). From those simulations that are consistent with the observed surface warming and ocean heat uptake, we can only derive a very broad probability density function (PDF) for the climate sensitivity (see Supplementary Information) which excludes neither very small climate sensitivities (around 1.2 K, the value if no feedbacks are present) nor unreasonably large values far above the widely accepted IPCC maximum of 4.5 K. This result is in agreement with recent PDF estimates for climate sensitivity, based on the observed surface warming, natural variability and either ocean models[16,17] or observed ocean warming[18,19]. This indicates that given the uncertainties in the radiative forcing, in the temperature records, and in currently used ocean models, it is impossible at this stage to strongly constrain the climate sensitivity, as proposed by Barnett *et al.*[10]. However, we can strongly constrain the sum of the radiative forcing and thereby the indirect aerosol forcing, the most uncertain of the individual forcing components. If we demand consistency with the temperature records, the PDF of the total radiative forcing for the year 2000 is considerably narrowed (1.4–2.4 $W m^{-2}$ for the 5–95% confidence range, Fig. 2b), compared to the initially assumed PDF (Fig. 2a). Furthermore, all results from comprehensive 3D climate models suggest a range for the climate sensitivity of about 1.5 to 4.5 K (ref. 1). By adopting this range as an additional constraint, which is completely independent of this study, a narrower forcing range results (1.6–2.5 $W m^{-2}$, Fig. 2c). Assuming the PDFs for the other forcing components to be correct estimates, the procedure reduces the initially assumed uniform PDF for the indirect aerosol forcing (Fig. 2d) considerably. Our analysis suggests that the negative indirect aerosol forcing plus any forcing not explicitly considered for the year 2000 is smaller than 1.2 $W m^{-2}$ in magnitude with a probability of 95% (Fig. 2e) for any climate sensitivity, and over 99% if the climate sensitivity is restricted to 1.5 K–4.5 K (Fig. 2f). Even for much less restrictive assumptions regarding the forcing PDFs, these probabilities decrease only slightly to 85% and 95%, respectively (for example, when all IPCC uncertainties are taken as one standard deviation and/or when using a broader PDF for the indirect aerosol forcing). Further simulations suggest that a slightly positive indirect aerosol forcing (plus any forcing not considered) at year 2000 cannot be excluded by this method, if the corresponding PDF assumption is extended to positive values. But although the uncertainty about its magnitude is large, there is general agreement that the indirect aerosol forcing is indeed negative[1].

A key question is whether the observed warming of the twentieth century does constrain the uncertainties in projections of future warming. We investigated the range of projected surface warming until the year 2100 for two illustrative emission scenarios of the IPCC, B1 and A2 (ref. 20), using only those simulations that are consistent with the temperature observations (Fig. 3a). If the observed surface warming and ocean heat uptake are taken as the only constraints, we find a surface temperature increase of 1.6 to 3.8 K (5–95% range, relative to the 1961–90 period) by the year 2100 for scenario B1 (Fig. 3b), with a probability of 40% that the warming exceeds the range given by the IPCC and <5% for a warming below that range. For a restricted range of climate sensitivities (1.5–4.5 K), we estimate 5–95% ranges for the projected warming of 1.5–2.6 K for scenario B1 (Fig. 3c), and 2.5–4.3 K (Fig. 3d) for A2, consistent with the results proposed by the IPCC for these scenarios and based on comprehensive 3D models.

These results are remarkable for several reasons. First, there is no

tuning of the simplified model towards more complex models. Thus, our results support the use of simplified models to assess the probabilities and uncertainties of the projections of at least global properties obtained by more complex models. Second, the IPCC results are obtained using different models but a single radiative forcing evolution for a certain scenario. Here we circumvent this limitation, and consider uncertainties in climate sensitivities, ocean mixing, and the reconstructed or projected radiative forcing. Third, taking the observed warming of ocean and atmosphere as the only constraint, we find that the currently accepted IPCC consensus about the uncertainty in global warming projections might significantly underestimate the probability of a strong warming. Our results are in agreement with the IPCC uncertainty ranges only when using a model-derived upper limit of about 5 K as an independent constraint for climate sensitivity. Whereas the IPCC attaches no statistical information to its projection uncertainties, the ensemble approach presented here suggests that the probability distribution of the temperature increase for a certain scenario is similar to a gaussian distribution, whose 5–95% range corresponds to the uncertainties given by the IPCC. The consistency with the observed warming is a strong constraint in our ensemble simulations for at least the next few decades, when the forcing is the main uncertainty. By the end of the century, the projection uncertainty for a particular scenario becomes increasingly dominated by the uncertainty in climate sensitivity.

The simplicity of our model prevents us from taking into account any internal variability of the climate system. We might therefore miss some nonlinear feedbacks, but we benefit from the fact that there is no noise superimposed on the model response. Another powerful method of scaling future climate projections is to use an optimal fingerprint method[11,12]. This method considers natural variability and does not require an estimate for climate sensitivity, but cannot take into account model and input uncertainties in a probabilistic way. Furthermore, the necessary assumption that the current balance of greenhouse warming and sulphate cooling remains approximately constant makes that method particularly useful for the near future, but not for long-term projections where sulphate forcing is expected to decrease substantially. The temperature ranges derived by this fingerprint method[11] for a similar scenario (IS92a) are consistent with our results, from which we conclude that including natural variability would not strongly widen the PDF for long-term temperature changes. We deliberately refrain from an overall probabilistic estimate by combining results from different emission scenarios[13], as that would depend on a subjective estimate of the likelihood of individual scenarios[2].

The combination of observed surface air temperature increase and ocean heat uptake with results from ensemble climate simulations provides a strategy to estimate more objectively uncertainties of climate projections. It is desirable that the present results be assessed by ensemble simulations with more comprehensive climate models. Further progress will depend on continuing high-quality observations with global coverage, in particular ocean temperatures, a refined understanding of the climate system, and significantly increased computational resources. □

Methods

The applied climate model consists of a zonally averaged dynamical ocean model, coupled to a zonally and vertically averaged energy- and moisture-balance model of the atmosphere[21,22]. For efficiency, we use the annual-mean model version, but differences from the results obtained with the seasonal version[23] are negligible. Whereas the climate sensitivity of comprehensive models is determined by the strength of the resolved feedback mechanisms, we specify the radiative perturbation at the tropopause as $\Delta F(t) = \Delta F_{RF}(t) + \lambda \Delta T_s(t)$, where ΔF_{RF} is the radiative forcing[1]. Feedback processes are parameterized in terms of the global-mean surface temperature increase ΔT_s, and the constant factor λ is prescribed to obtain different climate sensitivities[24]. We diagnose the climate sensitivity after 3,000 years of integration. The time history of radiative forcing is prescribed from changes in well-mixed greenhouse gases (CO_2, CH_4, N_2O, SF_6 and 28 halocarbons including those controlled by the Montreal Protocol), stratospheric and tropospheric O_3, the direct forcing of black and organic carbon and sulphate, stratospheric H_2O owing to CH_4 changes, and the indirect effects of aerosols, all based on simplified expressions that are summarized in refs 1 and 25. Anthropogenic radiative forcing is prescribed from reconstructions for the time 1765–2000, follows a SRES scenario[20] from 2000 to 2100, and is kept constant thereafter. For the simulations in Fig. 1, a standard value of -0.8 $W m^{-2}$ is assumed for the indirect aerosol forcing at year 2000, as in earlier studies[26]. Radiative forcing by volcanoes and variations in solar irradiance are prescribed for the historical period[27]. Albedo changes due to land use, radiative forcing by dust and the uncertainty in converting future greenhouse-gas emissions into concentrations[25] are not considered.

For the Monte Carlo simulations, we have calculated 25,000 global warming simulations using five ocean model set-ups and taking into account the uncertainties in radiative forcings and climate sensitivity. For each forcing component of every individual simulation, a random number (representing the radiative forcing for year 2000) is determined, to which the time history and future projection of that forcing component is scaled. These random numbers are chosen in such a way that their distribution follows the prescribed PDF of the forcing for the year 2000. A gaussian PDF is assumed where absolute uncertainties are given, a log-normal PDF where the uncertainty is expressed as a factor. We assume the uncertainties given by IPCC to be two standard deviations, although the IPCC attaches no statistical meaning to them. For the indirect aerosol forcing, the probability is assumed to be uniform between 0 and $-2\,W m^{-2}$ (see refs 25 and 28 for details about the radiative forcing assumptions). For each simulation, a climate sensitivity is randomly chosen between 1 and 10 K (uniform PDF).

An individual model simulation is considered to be consistent with observations if the simulated differences in both global-mean surface temperature between 1900 and 2000 and ocean heat content between 1955 and 1995 match observations within their uncertainties (two standard deviations) and if a correlation criterion indicates reasonable time-dependent agreement for both surface warming and ocean heat uptake.

Specifically, we divide the difference of the observed and modelled warming by the uncertainty of the observed warming (thereby expressing the model mismatch in terms of observation uncertainties), average over time and prescribe a maximum value for this quantity. The main conclusions do not depend on the exact choice of the consistency criteria. However, we implicitly assume that the long-term trends in observed surface warming and ocean heat uptake are due to natural and anthropogenic forcings, and that internal variability only contributes to decadal changes. Further, the results of this study are only weakly sensitive to the assumed forcing PDFs and ocean mixing properties, as unrealistic input/model combinations due to less restrictive input assumptions are usually eliminated by the observational constraints. For example, the indicated limits of surface temperature ranges at year 2100 change by less than ±0.2 K when assuming different ocean model versions or less restrictive PDFs of the radiative forcing.

Received 27 December 2001; accepted 22 February 2002.

1. Houghton, J. T. *et al.* (eds) *Climate Change 2001: The Scientific Basis* (Cambridge Univ. Press, Cambridge, 2001).
2. Schneider, S. H. What is 'dangerous' in climate change? *Nature* **411,** 17–19 (2001).
3. Jones, P. D., New, M., Parker, D. E., Martin, S. & Rigor, I. G. Surface air temperature and its changes over the past 150 years. *Rev. Geophys.* **37,** 173–199 (1999).
4. Levitus, S., Antonov, J. I., Boyer, T. P. & Stephens, C. Warming of the world ocean. *Science* **287,** 2225–2229 (2000).
5. Santer, B. D. *et al.* A search for human influences on the thermal structure of the atmosphere. *Nature* **382,** 39–46 (1996).
6. Tett, S. F. B., Stott, P. A., Allen, M. R., Ingram, W. J. & Mitchell, J. F. B. Causes of twentieth-century temperature change near the Earth's surface. *Nature* **399,** 569–572 (1999).
7. Stott, P. A. *et al.* External control of 20th century temperature by natural and anthropogenic forcing. *Science* **290,** 2133–2137 (2000).
8. Hegerl, G. C. *et al.* Optimal detection and attribution of climate change: sensitivity of results to climate model differences. *Clim. Dyn.* **16,** 737–754 (2000).
9. Stott, P. A. *et al.* Attribution of twentieth century temperature change to natural and anthropogenic causes. *Clim. Dyn.* **17,** 1–21 (2001).
10. Barnett, T. R., Pierce, D. W. & Schnur, R. Detection of anthropogenic climate changes in the world's oceans. *Science* **292,** 270–274 (2001).
11. Allen, M. R., Stott, P. A., Mitchell, J. F. B., Schnur, R. & Delworth, T. L. Quantifying the uncertainty in forecasts of anthropogenic climate change. *Nature* **407,** 617–620 (2000).
12. Allen, M. R. *et al.* Quantifying anthropogenic influence on recent near-surface temperature change. *Surv. Geophys.* (in the press).
13. Wigley, T. M. L. & Raper, S. C. B. Interpretation of high projections for global-mean warming. *Science* **293,** 451–454 (2001).
14. Hansen, J., Russell, G., Lacis, A., Fung, I. & Rind, D. Climate response times: Dependence on climate sensitivity and ocean mixing. *Science* **229,** 857–859 (1985).
15. Levitus, S. *et al.* Anthropogenic warming of Earth's climate system. *Science* **292,** 267–270 (2001).
16. Forest, C. E., Allen, M. R., Stone, P. H. & Sokolov, A. P. Constraining uncertainties in climate models using climate change detection techniques. *Geophys. Res. Lett.* **27,** 469–572 (2000).
17. Andronova, N. & Schlesinger, M. E. Objective estimation of the probability distribution for climate sensitivity. *J. Geophys. Res.* **106,** 22605–22612 (2001).
18. Gregory, J. M., Stouffer, R. J., Raper, S. C. B., Stott, P. A. & Rayner, N. A. An observationally based estimate of the climate sensitivity. *J. Clim.* (submitted).
19. Forest, C. E., Stone, P. H., Sokolov, A. P., Allen, M. R. & Webster, M. D. Quantifying uncertainties in climate system properties with the use of recent climate observations. *Science* **295,** 113–117 (2002).
20. Nakićenović, N. *et al. Special Report on Emission Scenarios* (Intergovernmental Panel on Climate Change, Cambridge Univ. Press, 2000).
21. Stocker, T. F., Wright, D. G. & Mysak, L. A. A zonally averaged, coupled ocean-atmosphere model for paleoclimate studies. *J. Clim.* **5,** 773–797 (1992).
22. Schmittner, A. & Stocker, T. F. The stability of the thermohaline circulation in global warming experiments. *J. Clim.* **12,** 1117–1133 (1999).
23. Schmittner, A. & Stocker, T. F. A seasonally forced ocean-atmosphere model for paleoclimate studies.

J. Clim. **14,** 1055–1068 (2001).
24. Plattner, G.-K., Joos, F., Stocker, T. F. & Marchal, O. Feedback mechanisms and sensitivities of ocean carbon uptake under global warming. *Tellus B* **53,** 564–592 (2001).
25. Joos, F. *et al.* Global warming feedbacks on terrestrial carbon uptake under the IPCC emission scenarios. *Glob. Biogeochem. Cycles* **15,** 891–907 (2001).
26. Kattenberg, A. *et al.* in *IPCC Second Scientific Assessment of Climate Change* (eds Houghton, J. T. *et al.*) 285–357 (Cambridge Univ. Press, Cambridge, 1996).
27. Crowley, T. J. Causes of climate change over the past 1000 years. *Science* **289,** 270–277 (2000).
28. Boucher, O. & Haywood, J. On summing the components of radiative forcing of climate change. *Clim. Dyn.* **18,** 297–302 (2001).
29. Knutti, R., Stocker, T. F. & Wright, D. G. The effects of subgrid-scale parameterizations in a zonally averaged ocean model. *J. Phys. Oceanogr.* **30,** 2738–2752 (2000).

Supplementary Information accompanies the paper on *Nature's* website (http://www.nature.com).

Acknowledgements

We thank T. Crowley for providing the volcanic and solar radiative forcing data. This work was supported by the Swiss National Science Foundation.

Competing interests statement

The authors declare that they have no competing financial interests.

Correspondence and requests for materials should be addressed to T.F.S. (e-mail: stocker@climate.unibe.ch).

Origins and estimates of uncertainty in predictions of twenty-first century temperature rise

Peter A. Stott* & J. A. Kettleborough†

* *Hadley Centre for Climate Prediction and Research, Met Office, Bracknell, Berkshire RG12 2SY, UK*
† *Space Science and Technology Department, Rutherford Appleton Laboratory, Didcot, Oxfordshire OX11 0QX, UK*

Predictions of temperature rise over the twenty-first century are necessarily uncertain, both because the sensitivity of the climate system to changing atmospheric greenhouse-gas concentrations, as well as the rate of ocean heat uptake, is poorly quantified[1,2] and because future influences on climate—of anthropogenic as well as natural origin—are difficult to predict[3]. Past observations have been used to help constrain the range of uncertainties in future warming rates, but under the assumption of a particular scenario of future emissions[4]. Here we investigate the relative importance of the uncertainty in climate response to a particular emissions scenario versus the uncertainty caused by the differences between future emissions scenarios for our estimates of future change. We present probabilistic forecasts of global-mean temperatures for four representative scenarios for future emissions[5], obtained with a comprehensive climate model. We find that, in the absence of policies to mitigate climate change, global-mean temperature rise is insensitive to the differences in the emissions scenarios over the next four decades. We also show that in the future, as the signal of climate change emerges further, the predictions will become better constrained.

An estimate of the uncertainty in a climate-model-based prediction of twenty-first century global-mean temperature rise is a potentially valuable tool for policy makers and planners[3,6,7]. Large and difficult-to-quantify uncertainties surround predictions of future demographic changes, economic development and technological change, which will determine future anthropogenic emissions of greenhouse gases and other pollutants. Even with perfect knowledge of emissions, uncertainties in the representation of atmospheric and oceanic processes by climate models limit the accuracy of any estimate of the climate response. Natural variability, generated both internally and from external forcings such as changes in solar output and explosive volcanic eruptions, also contributes to the uncertainty in climate forecasts.

Recently a technique has been developed to quantify uncertainty in predictions by comparing simulations of past temperature changes with observations[4]. Under this approach, based on those developed for the detection and attribution of climate change[8,9], we estimate the factors (with associated uncertainties) by which the model's simulated response to various external forcings over the twentieth century can be scaled up or down while remaining in agreement with the observations. The most important external forcings are well-mixed greenhouse gases, other anthropogenic pollutants such as sulphate aerosols (which are produced by oxidation of sulphur dioxide), changes in tropospheric ozone (which is controlled by photochemical reactions), stratospheric ozone depletion, and natural external forcings such as variations in solar irradiance and stratospheric aerosol from volcanic eruptions.

Temperatures will fluctuate about their mean climatic state owing to natural internal variability. We include decadal variability in our uncertainty analysis, but we do not consider sub-decadal variations that would be additional to the uncertainty in decadal temperatures presented here. We also consider fluctuations due to potential future changes in solar output and volcanic eruptions. As it is not possible to predict deterministically changes in natural forcings, we estimate natural external variability from simulations of the past 140 years that include these natural forcings.

The IPCC, in their Special Report on Emissions Scenarios (SRES[5]), has developed a wide range of future emissions scenarios, based on a variety of narrative 'storylines', each describing a possible future development of population, economies and energy sources. The range of scenarios includes interventions leading to reductions in sulphur emissions and introduction of new energy technologies, but does not include additional initiatives to mitigate climate change. Any estimate of socio-economic trends over the course of the twenty-first century is necessarily very uncertain and highly subjective. Our interest here lies in determining the range of likely future climates consistent with current observations under a representative range of emissions scenarios, and investigating how this uncertainty range will change as the signal of climate change becomes stronger.

We can address these questions with predictions of a coupled atmosphere–ocean general circulation model (AOGCM) using a representative subset of emissions scenarios which span most of the total SRES range, without assigning relative probabilities to the different emissions scenarios. On the assumption that a model that over- or under-estimates the climate response by a certain fraction now will continue to over- or under-estimate it by a similar fraction in the future, we can use a comparison between simulated and observed changes over the past 100 years to calculate the uncertainty in a prediction (according to a particular emissions scenario) over the next 100 years. This assumption appears to be justified for global-mean temperature by the AOGCM runs currently available, all of which evolve similarly over time in response to a given forcing despite differences in sensitivity and thus response amplitude[10]. Even though climate sensitivity is not well constrained by the observed temperature record[4,11], perturbation analysis of simple[4] and intermediate-complexity[11] models indicates that there is a generally linear relationship between past and future global temperature change as we vary the sensitivity of a climate model that continues to hold for unmitigated forcing until the end of the century[12], provided the climate sensitivity and sulphate aerosol forcing are not outside the likely range estimated by the IPCC